ORIGINAL PAPER

Assessment of solar PV potential and performance of a household system in Durban North, Durban, South Africa
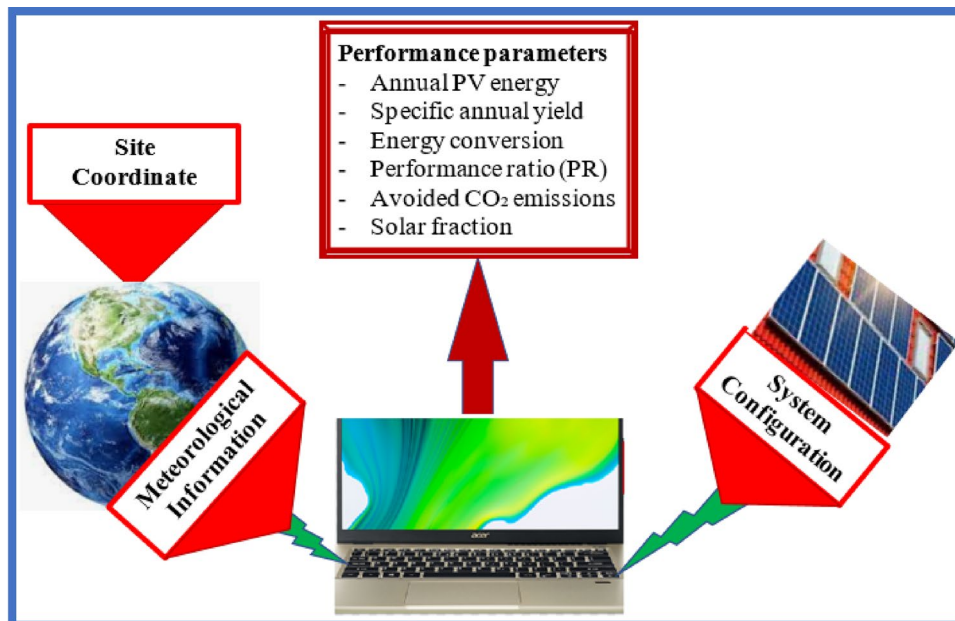
Williams S. Ebhota[1] [ID] · **Pavel Y. Tabakov[1]**

Abstract
The potential of solar PV is location-dependent that needs to be assessed before installation. This study focuses on the assessment of a solar PV potential of a site on coordinates −29.853762°, 031.00634°, at Glenmore Crescent, Durban North, South Africa. In addition, it evaluates the performance of a 6-kWp installed capacity grid-connected rooftop solar PV system to supply electricity to a household. The results, obtained from PV design and simulation tools—PV*SOL, Solargis prospect, and pvPlanner, were used to analyze and establish the PV system's economic and technical viability. The configuration of the system is as follows: load profile—a 2-person household with 2-children, energy consumption—3500 kWh, system size—6 kWp, installation type—roof mount, PV module type—c-Si—monocrystalline silicon, efficiency—18.9%, orientation of PV modules -Azimuth 0° and Tilt 30°, inverter 95.9% (Euro efficiency), and no transformer. The results show: meteorological parameters—global horizontal irradiation (GHI) 1659.3 kWh/m^2, direct normal irradiation (DNI) 1610.6 kWh/m^2, air temperature 20.6 °C; performance parameters—annual PV energy 8639 kWh, Specific annual yield 1403 kWh/kWp, performance ratio (PR) 74.9%, avoided CO_2 emissions 5662 kg/year, and solar fraction 42.5%. Others are economic performance parameters—levelised cost of energy (LCOE) 0.1147 USD/kWh, internal rate of return (IRR) 17,671 USD/kWh, and return on investment (ROI) 11%. The results show that the proposed solar PV system under the current conditions is both economically and technically viable for household electrification in Durban North, South Africa.

Graphical abstract

Extended author information available on the last page of the article

Abbreviations

ALB	Surface albedo
CAPEX	Capital expenditure
CDD	Cooling degree days
CF	Capacity factor
D2G	Ratio of diffuse horizontal irradiation and global horizontal irradiation
DIF	Diffuse horizontal irradiation
DNI	Direct normal irradiation
GHI	Global horizontal irradiation
GTI	Global tilted irradiation
HDD	Heating degree days
IRR	Internal rate of return
LCOE	Oevelised cost of energy
NPV	Net present value
OPEX	Operating expenses
PPA	Power purchase agreement
PR	Performance ratio
PREC	Precipitation
PV	Photovoltaic
PVOUT	Photovoltaic power output
PWAT	Precipitable water
RH	Relative humidity
ROI	Return on investment
SNOWD	Snow days
TEMP	Air temperature
WS	Wind speed
$Dir_{\theta,\alpha}$	Direct insolation from the sun map
θ	Centroid at zenith angle
α	Azimuth angle
S_{Const}	Solar constant
β	Transmissivity of the atmosphere
$SunDur_{\theta,\alpha}$	Time duration represented by the sky sector
$SunGap\theta,\alpha$	Gap fraction for the sun map sector
$m(\theta)$	Is the relative optical path length
$AngIn\theta,\alpha$	Angle of incidence between the centroid of the sky sector and the axis normal to the surface
G_z	Is the surface zenith angle
G_a	Is the surface azimuth angle
θ_1 and θ_2	Bounding zenith angles Sky sector
Div_{azi}	Number of azimuthal divisions in the sky map
$PV_{OUTspecific}$	Specific photovoltaic power output
G_i	Mum of direct, diffuse, and ground-reflected irradiance incident
H_i	In-plane irradiation
E_{out}	Energy output
P_o	Array power rating
L_c	Array capture losses
Y_R	Reference yield
Y_F	Array yield
G_{CC}	Clean reference solar cell irradiance
G_{DC}	Dirty reference solar cell irradiance
GL	Soiling loss

Introduction

The continuous extensive use of fossil fuels is increasingly adding to the concentration of CO_2 in the atmosphere, which contributes to the global temperatures rise and environmental degradation (Almasoud and Gandayh 2015). The use of fossil fuel contributes the highest share to CO_2; a by-product of fossil fuel combustion, emitted into the atmosphere (Nachmany et al. 2014). The sacrificing of the environment and human health for the energy required for socio-economic activities continues. The International Energy Agency (IEA), reported that the global energy-related CO_2 emissions in 2019 was 33.4 $GtCO_2$ and dropped to 31.5 $GtCO_2$ in 2020 because of pandemic (IEA 2021). About 38.5% of the global CO2 emissions come from the power sector (Worldmeter 2020). South Africa emitted about 456 MtCO2 and contributed 1.3% of the global CO_2 emissions. The country ranked was 1st and 14th emitter of CO_2 in Africa and the world, respectively (Fleming 2019); about 60.5% of the emission comes from the power sector (Worldmeter 2021).

The present large economies are products of fossil fuels, such as natural gas, coal, and oil. These are unarguably effective economic boosters, but they leave behind negative environmental impacts and health consequences (Ebhota and Tabakov 2020). The consequential effects of the continuous use of these fuels to the biosphere (FloodList 2019a, b; Aljazeera 2019) are evidenced in the increasing climate change triggered events. Some of these events are the unceasing rise in temperatures, droughts, floods, cyclones, storms and ice melts, and migration. Unfortunately, the compromise that follows the provision of energy for economic activities has not bridged the gap of energy insufficiency in many developing countries. About 50% of the population in 41 countries in sub-Saharan Africa (SSA) has no adequate access to energy; 650 million people are expected not to have access to power by 2030 (IEA 2017).

Apart from environmental and health issues caused by fossil fuels, the depletion of fossil fuels and the unabated price fluctuations is turning urgent attention to energy conservation. In this regard, several efforts have been advanced to check the environment and health issues associated with

energy generation and consumption. These include measures to reduce energy consumption, maximisation of the use of renewable energy (RE), use of hybrid renewable energy systems (HRES) (Rinaldi et al. 2021), digitalization, and decentralisation of energy systems (DCES), and the smart grid. In the same vein, the deployment of solar photovoltaic (PV) systems is increasing and due to the continuous decline of solar PV components prices. In addition, the utilisation of solar energy mitigates climate change consequences, promotes a decentralisation system, reduces the dependence on energy imports, and has extensive grid infrastructure.

The need for alternative energy

The decision by the United Nations (UN) to cut down the global consumption of fossil fuel, to reduce the effect of CO_2 emissions was well-received globally (UN 2015). However, there is a need to develop alternative energy sources to replace fossil fuel; since energy is what powers socioeconomic growth. These alternatives are expected to be clean, reliable, adequate, and affordable energy. Sustainable energy transition will simply be fiction or a mirage without alternative energy to replace fossil fuel (Ebhota 2019; Ebhota and Jen 2018). Subsequently, the contemporary questions surrounding energy are centered on how to harness RE resources; raise the efficiency of supply and end-use; reduce CO_2 emissions originating from energy generation and consumption; provide clean energy for all. This implies that much advancement has to be made to improve and facilitate RE deployment. Renewable energy technologies such as solar, biofuels, hydro, geothermal, tidal, and wind are currently receiving massive interest in terms of deployment, investment, and research and development. In addition, nuclear energy has also been described as reliable, safe, clean, compact, competitive, and practically inexhaustible (Eiden 2014). However, because of the perceived side effects, many countries are skeptical about the use of energy although nuclear has enormous energy required for electricity.

Solar energy

Amongst the three most harnessed RE resources (solar, small hydropower, and wind), solar photovoltaic is the most deployed. This is mainly because of its widespread availability coupled with the continuous price decline of PV components, easy installation, and low maintenance cost. Solar energy is regional dependent and the annual direct solar irradiation in some regions exceeds 300 Watt per square meter (W/m^2). A study observed that many of the countries that are likely to experience a rapid increase in urbanisation are in solar-rich regions, such as Singapore, Nigeria, Spain, Australia, India, and South Africa (WEC 2013). This gives solar PV systems

the greatest potential for wider utilisation in SSA. Singapore is already exploiting the PV system, and has planned to raise solar power through a roadmap that adopts two scenarios—a "baseline" (BAS) scenario and an "accelerated" (ACC) scenario (Roadmap 2020). The targets of these scenarios are BAS—1 GWp and 2.5 GWp by 2030 and 2050, respectively; ACC—2.5 GWp and 5 GWp by 2030 and 2050, respectively. The success of this plan will save the yearly CO_2 emissions of about 1.6 million tonnes (Mt) and 3.4 Mt by 2030 and 2050, respectively. The realisation of the significance of the massive deployment of the different scales of solar PV systems in SSA will help to address the frequent blackouts and inadequate power supply considerably. At the same time, it would facilitate the building of a sustainable energy system in the end, which will reduce CO_2 emissions (Njoku and Omeke 2020).

Despite the successes recorded in solar efficiency, structure, and cost, the efficiency of multi-crystalline silicon photovoltaic (PV) cells is hovering around 10% to 17% (Kammen and Sunter). Recently, PV laboratory studies have reported efficiency of over 40%, using concentrated multi-junction cells (NREL 2016). Researches are ongoing to further improve the PV panel conversion performance and cost decline. Solar power is location depended, hence, this study provides PV potential and system information required for reliable and optimised solar PV systems at a location in Glenmore Crescent, Durban.

The goal of this study is to assess the solar PV Potential and performance of a 6-kWp system grid-connected for a household in site at Durban North, Durban, South Africa. The study is expected to provide information that will facilitate accurate PV system sizing and offer both economic and technical guides to installers and investors. Additionally, policymakers will find this study useful in forming the relevant framework to boost the provision of clean electricity. The objectives of this study include evaluation of the yearly average:

1. Global horizontal irradiation (GHI)
2. Direct normal irradiation (DNI)
3. Diffuse horizontal irradiation (DIF)
4. Global tilted irradiation (GTI)
5. Ambient temperature (TEMP)
6. Specific photovoltaic power output (PVOUT specific)
7. Total photovoltaic power output (PVOUT total)
8. Performance ratio (PR)

Background of study

Solar resource basics and modeling solar radiation

Solar radiation is used to assess the potential power levels that can be generated from photovoltaic cells and is

necessary for determining cooling loads for buildings. Hence, accurate quantification of solar radiation is required for various PV system applications, such as agricultural and water resource planning, management, and the design of irrigation systems. Additionally, solar radiation is the most basic and reliable renewable and clean energy source in nature that can play an alternative role to fossil fuels. Therefore, the knowledge of solar radiation is essential for the optimal design and evaluation of solar energy applications, such as photovoltaic and solar-thermal systems. Solar radiation takes a reasonable time before it reaches the Earth's surface, causing it to have various extra-terrestrial interactions with the atmosphere and surfaces of objects along its path. The amount of solar radiation per unit of horizontal area for a given locality is called, insolation, it originates from the sun, and depends mainly on the distance between the earth and sun, and solar zenith angle. Insolation can also be altered by the atmosphere, topography, and surface features, as it travels down the earth. At the earth's surface, it forms three radiation components, as shown in Fig. 1—direct, diffuse, and reflected radiations—the direct radiation makes a direct line from the sun as it is intercepted by the earth unobstructed; the diffuse radiation is dispersed by atmospheric constituents, such as dust and clouds as it travels through them; and the reflected radiation hits on surface features along its path and gets reflected. The summation of these three radiation components is called global or total solar radiation.

Amongst these three components, direct radiation is the largest component, followed by diffuse radiation while the reflected radiation constitutes the least proportion, except for locations surrounded by highly reflective surfaces, such as snow-covered areas. The point locations or entire geographic area's radiation can be estimated using solar radiation tools and this involves the following four steps (Rich et al. 1994; Cioban et al. 2013; Alamoud 2000):
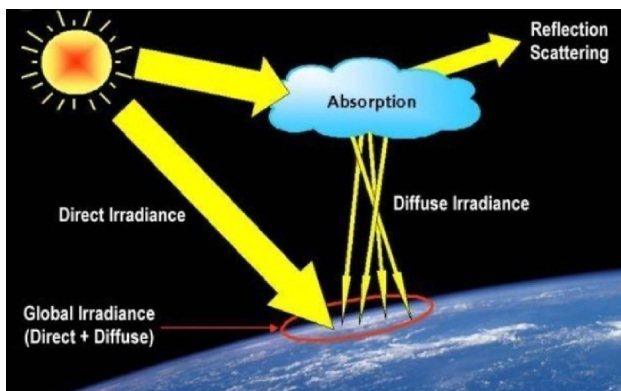
1. The computation of an upward-looking hemispherical viewshed based on topography.
2. Estimation of direct radiation by overlaying the viewshed on a direct sun map.
3. Estimation of diffuse radiation by overlaying the viewshed on a diffuse sky map

This process can be repeated for every location of interest to create an insolation map.

Mathematical calculation of insolation

The solar radiation analysis tools compute insolation throughout a landscape or for particular locations, center on techniques from the hemispherical view-shed algorithm created by Rich et al. (Rich et al. 1994; Fu and Rich 2002). The total radiation is computed for a specific location and is given as global radiation. The computation of direct, diffuse, and global insolation is replicated for every featured location on the topographic surface, creating insolation maps for the total geographical area.

Direct Normal Irradiation/Irradiance (DNI) is the element that deals with the photovoltaic concentration technology (concentrated photovoltaic, CPV) and thermal (concentrating solar power, CSP).

Global Horizontal Irradiation/Irradiance (GHI) is the summation of direct and diffuse radiation collected on a horizontal plane. GHI is used as the basis for climatic zones radiation comparison and is an essential parameter for computing radiation on a tilted plane.

Global Tilted Irradiation/Irradiance (GTI), or total radiation collected on a surface with set tilt and azimuth angles, fixed or sun-tracking is the summation of the direct, scattered, and reflected radiation. It is occasionally affected by shadow and is used for PV applications.

Global radiation calculation

The estimated global radiation ($Global_{tot}$) is (ArcMap 2020):

$$Global_{tot} = Dir_{tot} + Dif_{tot} \qquad (1)$$

where Dir_{tot} and Dif_{tot} are direct and diffuse radiation of all sun map and sky map sectors, respectively.

$$Dir_{tot} = \Sigma Dir_{\theta,\alpha} \qquad (2)$$

$$Dir_{\theta,\alpha} = S_{Const} * \beta^{m(\theta)} * SunDur_{\theta,\alpha} * SunGap_{\theta,\alpha} * \cos(AngIn_{\theta,\alpha}) \qquad (3)$$

where $Dir_{\theta,\alpha}$ is the direct insolation from the sun map sector ($Dir_{\theta,\alpha}$) with a centroid at zenith angle (θ) and azimuth angle (α); S_{Const} is the solar constant, and 1367 W/m^2 is usually

Fig. 1 Components of total/global radiation (direct, diffused, and reflected radiations) (Cotfas N/A)

used in the analysis; β is the transmissivity of the atmosphere; $m(\theta)$ is the relative optical path length; $SunDur_{\theta,\alpha}$ is the time duration represented by the sky sector; $SunGap\theta,\alpha$ is the gap fraction for the sun map sector; $AngIn\theta,\alpha$ is the angle of incidence between the centroid of the sky sector and the axis normal to the surface.

Relative optical length, $m(\theta)$, is function of solar zenith angle (θ) and elevation above sea level. For zenith angles less than 80°, relative optical length, $m(\theta)$:

$$m(\theta) = \text{EXP}\left(-0.000118 * \text{Elev} - 1.638 * 10^{-9} * \text{Elev}^2\right)/\cos(\theta) \tag{4}$$

Angle of incidence ($AngInSky_{\theta,\alpha}$):

$$\text{AngIn}_{\theta,\alpha} = \text{acos}\left(\text{Cos}(\theta) * \text{Cos}(G_z) + \text{Sin}(\theta) * \text{Sin}(G_z) * \text{Cos}(\alpha - G_a)\right) \tag{5}$$

where G_z is the surface zenith angle, and G_a is the surface azimuth angle.

Computation of diffuse radiation

The diffuse radiation at its centroid (D_{if}) is estimated, integrated over the time interval, and corrected by the gap fraction and angle of incidence utilizing this expression in (6):

$$\text{Dif}_{\theta,\alpha} = R_{glb} * P_{dif} * \text{Dur} * \text{SkyGap}_{\theta,\alpha} * \text{Weight}_{\theta,\alpha} * \cos\left(\text{AngIn}_{\theta,\alpha}\right) \tag{6}$$

where R_{glb} is the global normal radiation; P_{dif} is the proportion of the diffused global normal radiation flux (it is usually estimated 0.2 for very clear sky conditions and 0.7 for very cloudy sky conditions); D_{ur} is the time interval for analysis; $SkyGap_{\theta,\alpha}$ is the gap fraction for the sky sector (proportion of visible sky); $Weight_{\theta,\alpha}$ is the proportion of diffuse radiation starting from a given sky sector relative to all sectors; $AngIn_{\theta,\alpha}$ is the angle of incidence between the centroid of the sky sector and the intercepting surface.

The global normal radiation (R_{glb}) can be computed by summing up the direct radiation from every sector, without correction for angle of incidence, then correcting the proportion of direct radiation, which equals $1-P_{dif}$:

$$R_{glb} = \left(S_{\text{Const}}\Sigma\left(\beta^{m(\theta)}\right)\right)/\left(1 - P_{dif}\right) \tag{7}$$

$$\text{Weight}_{\theta,\alpha} = \left(\cos\theta_2 - \cos\theta_1\right)/\text{Div}_{azi} \tag{8}$$

where θ_1 and θ_2 are the bounding zenith angles of the sky sector; Div_{azi} is the number of azimuthal divisions in the sky map.

For the standard overcast sky model, $Weight_{\theta,\alpha}$ is computed as follows:

$$\text{Weight}_{\theta,\alpha} = \left(2\cos\theta_2 + \cos2\theta_2 - 2\cos\theta_1 - \cos2\theta_1\right)/4 * \text{Div}_{azi} \tag{9}$$

Total diffuse solar radiation for the location (Dif_{tot}) is computed as the sum of the diffused solar radiation (Dif) from all the sky map sectors:

$$\text{Dif}_{tot} = \Sigma\,\text{Dif}_{\theta,\alpha} \tag{10}$$

Solar PV system design and simulation applications

Many reliable and innovative software applications have been developed to carry out solar PV assessment, system design, costing, energy generation prediction, and operation activities. Other uses are obtaining PV site location and meteorological information, assessing the site's solar PV potential, and conducting system design, PV panel degradation assessment, and financial analysis. The impacts of the sun on a geographic area of a given period can be mapped and analyzed using solar radiation analysis tools that exploit two methods:

1 Calculation of insolation across an entire landscape, in a repeated manner for each location in the input topographic surface, using area solar radiation tool landscape.
2 Calculation of the amount of radiant energy for a specified location, using the point's solar radiation tool.

In addition, they are used by solar installers for system design for stand-alone/off-grid, grid-connected, and hybrid systems for industrial plants, commercial, and residential buildings (Li 2021). Some of these applications and their uses are presented in Table 1.

Economics of rooftop solar PV system

The economic performance of the PV system depends on the following factors—the finance system, federal and local policies, utility rate, and level of technical potential available to the commercial PV rooftop. The evaluation of the financial benefits of a PV system requires an elaborate financial analysis to determine the levelised cost of energy (LCOE), return on investment (ROI), net present value (NPV), and internal rate of return (IRR). The IRR is the profit an investor gains in percentage form by investing in a solar PV system. The ROI offers a relatively simple view of how much money an investor will save over the total lifetime (usually 25 to 30 years) of a solar project.

There are two distinct merits of rooftop PV systems—power costs advantage and provision of clean electricity. The investment of rooftop is mostly through the operating expenses (OPEX) model or the capital expenditure (CAPEX) model. These are the commonest investment options. The operating expenses OPEX model involves the

Table 1 Software applications used for solar PV systems performance analysis (Dondariya et al. 2018; Fuzen 2021; Khatib et al. 2012)

Software	Software specifications	Inputs required
PV*SOL	It is applied for the Planning and simulation of a site-specific solar PV system	Location Coordinates, meteorological data, system and auxiliary devices requirements
SolarGIS	A satellite map-supported online simulation tool for site assessment, planning and optimization of solar PV systems, and comparing energy harvest from various PV technologies	Type of PV technologies, local coordinates, AC/DC losses, load demand, cable sizing
PVGIS	An open-source research tool for performance assessment of PV technology in geographical regions and as a support system for policymaking in the European union	Total irradiance, Monthly values of atmospheric conditions, the mounting position
SISIFO	An open web service software for simulation of PV systems	Location of the system, the solar resource data, technical characteristics of the system and optionally system economics
PVsys	A software application for the study, sizing, and data analysis of complete PV systems. The PV systems include stand-alone, grid-connected, pumping and DC-grid. The application has extensive metrological and PV systems components databases, as well as general solar energy tools	Site location, Albedo definition, some sizing conditions and parameters specific to a project

provision of PV systems by the developers and sell the generated energy to the consumer. It requires legally binding; a long-term agreement between the consumer and the rooftop solar system provider and power purchase agreement (PPA) must be signed. In the case of the CAPEX model, the consumer owns the project and bears the capital expenses incurred during the installation of a rooftop system upfront. These expenses include the cost of equipment and other installation material, set up, labor, maintenance, upgrades, and operating the project. Excess residential power generated can be delivered to the grid. The OPEX model has the benefit of going solar without having to spend large upfront investments. Under the CAPEX model, the consumer takes ownership, quality, and safety responsibilities, unlike the OPEX model that is own and run by a third party. There are compromises in quality caused by saving costs by the third party in the CAPEX model. The CAPEX model is relatively cheaper than the OPEX model and hence, recommended for retail players and small and medium-scale enterprises.

Levelised cost of energy

Levelised cost of energy is the approximated revenue required to generate and run a generator over a given period of cost recovery is called LCOE. That is, the generated electricity from a known source is sold at a price to break even over the project lifetime (Huld et al. 2014). This energy cost evaluation method is based on OPEX and CAPEX estimates (Wolf 2015). Levelised cost of energy is used to measure and compare alternative means of energy generation and determine the viability of an energy project. Equation (14) is used to estimate LCOE (Huld et al. 2014):

$$\text{LCOE} = \frac{\sum_{t=1}^{n} \frac{I_t + M_t + F_t}{(1+r)^t}}{\sum_{t=1}^{n} \frac{E_t}{(1+r)^t}} \tag{11}$$

where I_t is the investment expenses in year t; M_t is the maintenance and operations costs in year t; F_t is the fuel costs in year t and $t = 0$ zero for PV electricity; E_t is the electricity produced in the year t; r is the discount rate; and n is the investment period in years.

Considering CAPEX as a primary input in the calculation of LCOE, utilizing the available most harmonised data set, Eq. (12) can be used (ESMAP 2020):

$$\text{LCOE} = 1 \frac{\sum_{t=1}^{n} \frac{\text{CAPEX}_t + \text{OPEN}_t}{(1+r)^t}}{\sum_{t=1}^{n} \frac{\text{PVOUT}_t}{(1+r)^t}} \tag{12}$$

Methodology

The study involves the assessment of solar PV potential of Glenmore Crescent, Durban North, South Africa; estimation of the electricity generation capacity of the location; and model solar PV system. The study will exploit the geospatial technology of two PV software applications, PV*SOL and Solargis, to evaluate and present solar resource information, PV system design model, simulation, and optimization results. The software applications are supported with satellite-derived annual global solar radiation and temperature data. The assessment will be used to define the amount and pattern of solar insolation and the capacity of PV power that can be generated by the solar resource. This information will be inputted in the modeling of solar PV systems for the generation of electricity with net-zero or sub-zero CO_2
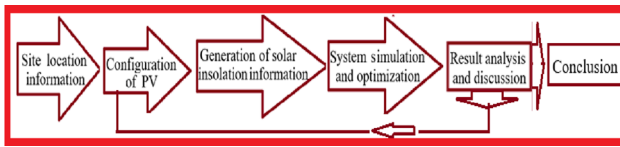
Fig. 2 Schematic of the methodology flowchart

Fig. 3 A section of Glenmore Crescent, Durban North, South Africa

emissions. The schematic diagram in Fig. 2 represents the flowchart of the methodology employed in this study.

Location information and system description

Detailed information of the site location is a requirement for an accurate solar PV potential estimation since the performance of the PV system depends on site-specific meteorological factors. These factors are wind speed, solar irradiance characteristics, and ambient temperature. Other determinants are installation site factors, which include dust, pollution level, latitude, orientation, and tree cover. The site is located in a residential area and a section of the site, as obtained from Google Map, is shown in Fig. 3.

For this study, a hypothetical household building was selected as a site, at a latitude of 29.800955°, the longitude of 31.0327245° in Glenmore Crescent, Durban North, South

Africa. Other information on the selected site is presented in Table 2.

Simulation of grid-connected PV system

The selection of the load profile, PV module, and installation types will be carried out using solar PV potential evaluator and design applications. Based on inputs optimisation considerations, the PV*SOL and Solargis software applications will be used to evaluate various parameters of a solar PV system, such as the daily, monthly, and yearly irradiations, terrain horizon, and day length, energy production, annual yield, and total system losses. In addition, a tabular comparative analysis of some critical solar system parameters overview will be presented. Generally, the grid-connected PV system is made up of solar PV panel arrays, a solar inverter, electrical panel, array mounting racks, cabling, meters, combiner box, surge protection, disconnects (array DC disconnect, inverter DC disconnect, inverter AC disconnect, exterior AC disconnect), and grounding equipment other electrical accessories, as shown in Fig. 4.

Simulation results and discussion

This section presents a detailed description of the load profile, configuration of the PV system, and the inputted parameters. It also includes simulation results presentation, analysis, and discussion of solar irradiations, energy production, annual yield, and total system losses.

The description of the system

The installation type used in this study is a rooftop mount, meaning that the 6 kW$_p$-installed capacity of the PV system was hypothetically mounted on a tilted roof of a residential building. The Azimuth and angle of tilt of the PV panels are harmonised such that the panels do not overlap or shade each other. The mounting of PV panels on rails that are attached

| Table 2 The site location and the system information	Site location information	
	Project name	Durban North
	Address	Glenmore Crescent, Durban North, South Africa
	Geographical coordinates (°)	−29.800955, 31.0327245
	Time zone	UTC+02, Africa/Johannesburg [SAST]
	Elevation (m)	48
	Land cover	Urban areas
	Population density (inh./km^2)	2892
	Terrain azimuth (°)	118
	Terrain slope (°)	3
	Annual air temperature at 2 m (°C)	20.9
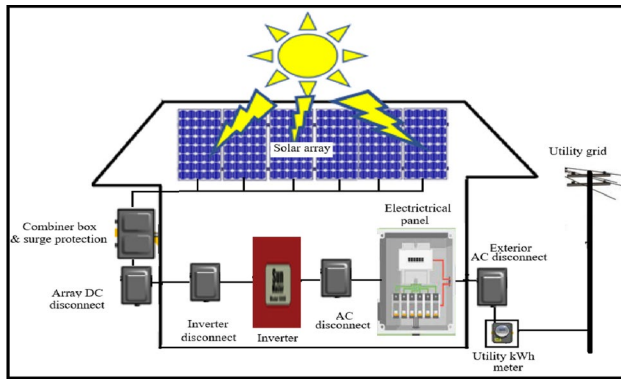
Fig. 4 Components of the grid-connected PV system (Roos, Nelson, and Brockman 2009)

to a tilted roof gives room for backside ventilation. A low-voltage grid connection, which is in a parallel circuit connection, through an inverter without storage is suitable for this type of PV system. Monocrystalline PV cell material was selected because of the quest for higher efficiency and the system is on a fixed stand type that can adequately power a household of a small family. Details of other inputs used in this study are presented in Table 3.

The potential solar resource—solar irradiation

Solar insolation fuels the PV power system, hence, is the most significant project-specific meteorological parameter that defines or boosts solar electricity generation. Solar irradiation was used professionally to evaluate the energy yield of a PV system site at Glenmore Crescent, Durban North. The estimates of solar monthly and yearly variations of GHI, DNI, and DIF of the selected site, as obtained from Solargis Prospect, are depicted in Fig. 5a and b, respectively. Durban North has GHI relatively high in seven months—from

January to March, and September to December and low for four months—April to August, as shown in Fig. 5a.

The highest irradiation of the site under consideration is in January; the results from Solargis Prospect and PV*SOL show 180 kWh/m2 at 24 °C and 190 kWh/m2 at 21 °C, respectively, as shown in Fig. 6a and b. The range of solar insolation received by the site throughout the year is from 95 to 190 kWh/m^2. The pattern of irradiance obtained, further strengthened the assertion that solar energy significantly depends on seasonal variation across the year.

Terrain horizon and day length

The length of a day is determined by the following factors—geographical latitude of the location, altitude of the sun, hour angle, and the sun declination angle. Figure 7a presents the horizon and sun path over a year in Durban North (the module horizon, terrain horizon, and active area with civil and solar time), which may have a shading effect on solar radiation. The change of day length and minimum zenith angle during a year are presented in Fig. 7b. The local day length (the time when the Sun is above the horizon) is shorter compared to the astronomical day length if obstructed by a higher terrain horizon.

Performance parameters

The sustenance of the ongoing development of the solar PV industry depends critically on the accurate PV system performance. The performance parameters are used to make comparisons of systems with different geographic locations, designs, and/or technology, and to allow operational problems detection. These parameters, which include performance ratio (PR), reference yield, final PV system yield, and Photovoltaics for utility-scale applications (PVUSA) rating, define the overall system performance concerning the solar resource, energy production, and total system losses effect

Table 3 System information

| Load profile	2-Person household with 2-children
Energy consumption (kWh)	3500
System size (kWp)	Installed capacity: 6
Installation type	Roof mount
PV module type (%)	c-Si—crystalline silicon (mono), efficiency 18.9
Geometry of PV modules (°)	Azimuth: 0; Tilt: 30
Inverter type (%)	Inverter 95.9 (Euro efficiency)
Transformer type	No transformer
Snow and soiling losses at PV modules (%)	Monthly soiling losses up to 4.5; Monthly snow losses up to 0.0
Cabling losses (%)	DC cabling 1; DC mismatch 0.8; AC cabling 0.2
Albedo	20
System availability (%)	97
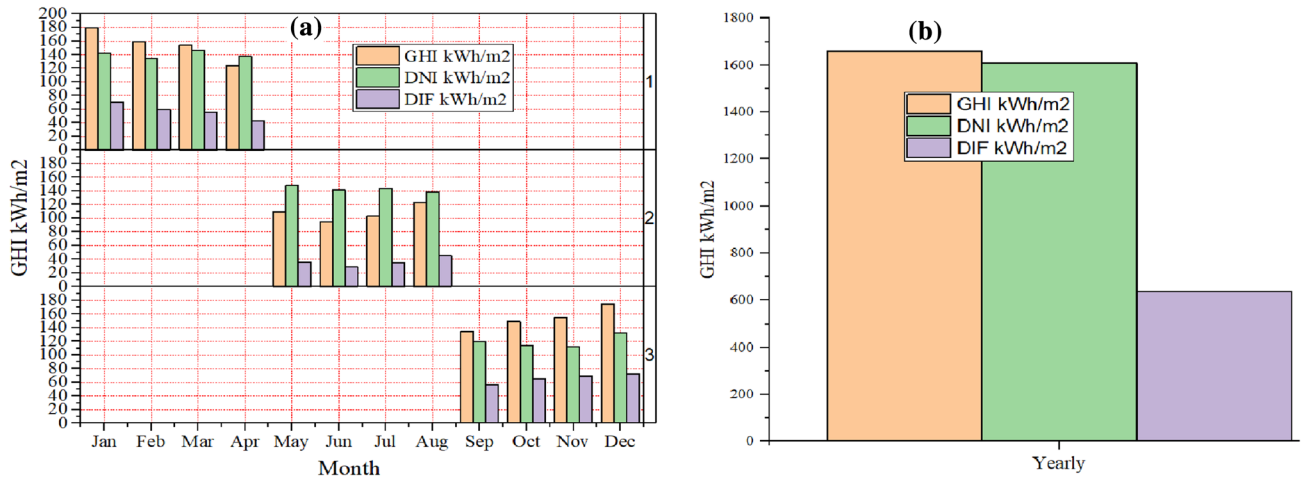
Fig. 5 The estimates of **a** solar monthly and **b** yearly variations of GHI, DNI, and DIF of Durban North
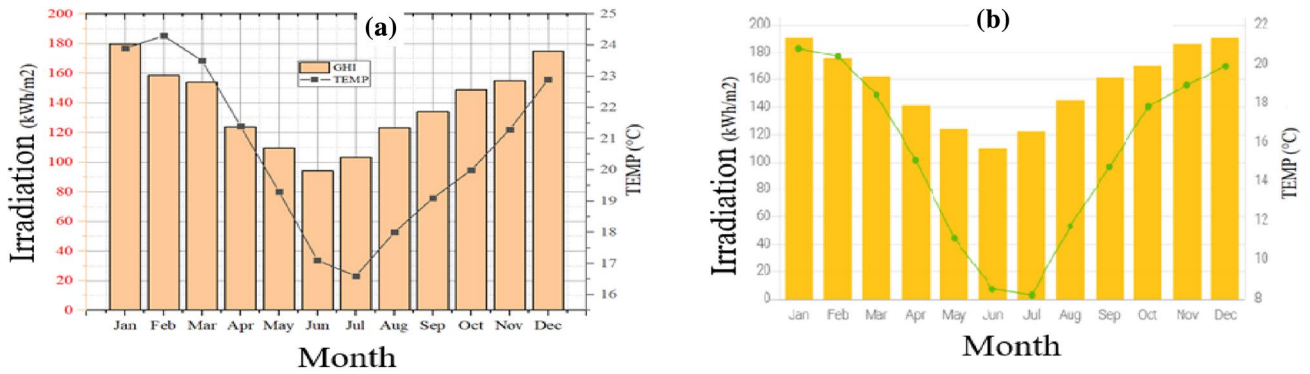

Fig. 6 Monthly irradiation and temperature data at Durban North, South Africa obtained from **a** Solargis; and **b** PV*SOL
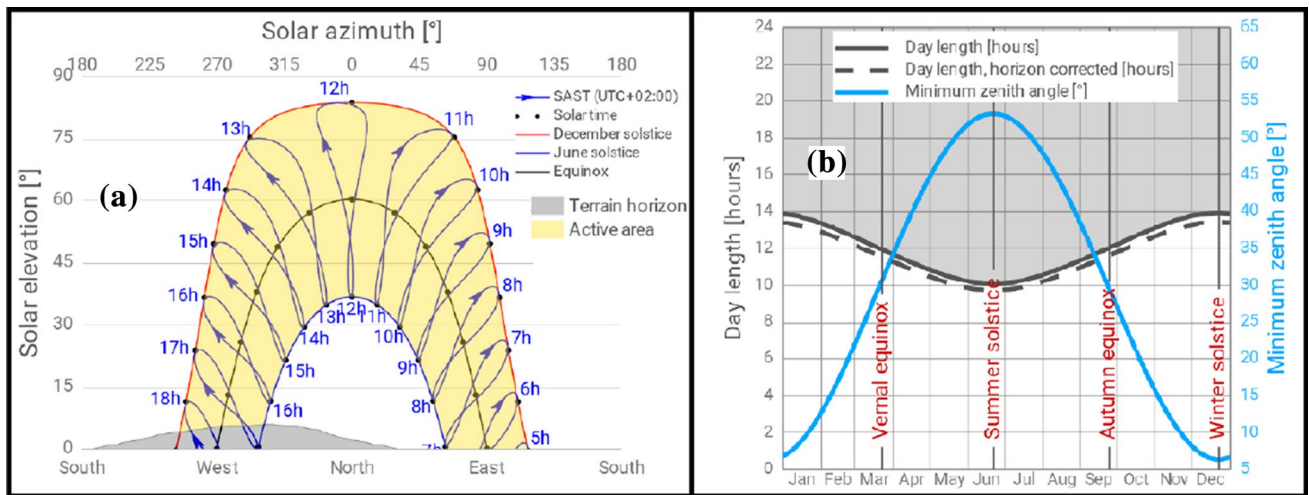

Fig. 7 **a** Path of the sun over a year in Surabaya; **b** Day length and solar zenith angle

(Marion et al. 2005). One of the most significant variables for estimating the efficiency of a PV plant is PV.

Performance ratio (PR)

The performance ratio is the ratio of the actual energy output and the possible theoretical energy output. It is mainly independent of the positioning of a PV plant and the incident solar irradiation on the PV plant. It is a measure of a PV system performance, taking into account meteorological factors, such as irradiation, climate changes, relative humidity (RH), and temperature. Hence, the PR can be used to compare PV plants supplying the grid at various locations all over the world.

The ratio between specific alternating current (AC) electricity output of a PV system and global tilted irradiation (GTI) obtained by the surface of a PV array, is termed as performance ratio (PR) (Quansah et al. 2017).

$$\text{PR} = \frac{\text{PV}_{\text{OUTspecific}}}{\text{GTI}} \qquad (13)$$

$$\text{PR} = Y_f/Y_r \qquad (14)$$

$$Y_f = \left(E_{\text{out}}/P_o\right) \qquad (15)$$

$$Y_r = \left(H_i/G_{i,\text{ref}}\right) \qquad (16)$$

where $PV_{OUTspecific}$ is the specific photovoltaic power output (kWh/kWp), G_i is the sum of direct, diffuse, and ground-reflected irradiance incident upon an inclined surface parallel to the plane of the modules in the PV array, H_i is the in-plane irradiation kWh/m^2, E_{out} is the Energy output from PV system (AC), (kWh); P_o, is the array power rating, AC, (kW).

The computation and report of PR are based on monthly or yearly output, although it can be calculated for smaller intervals, such as daily or weekly. This may be used to identify the occurrences of component failures. Because of losses due to PV module temperature, the values of PR in the winter are greater than in the summer, which usually falls within the range of 0.6 to 0.8. The maximum energy production is 1100 kWh in August, while the minimum is 810 kWh in February, as shown in Fig. 8. The reasons behind the high yield in August are the longest day of sunshine and low ambient temperature. The cloudy or rainy season is responsible for the low yield in February. Similarly, heavy electrical load, such as water geyser, and room heater connected to the system during winter accounts for the high-energy consumption (300 kWh) in July and August.
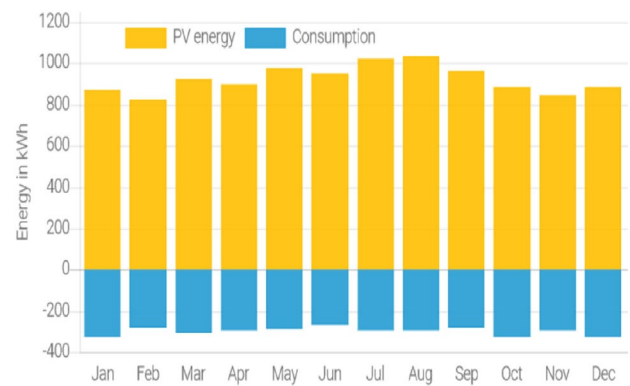

Fig. 8 Annual energy production and consumption

For the small household, the projected total energy consumption from the software is 3500 kWh. The PV system supplied 1502 kWh, about 43%, and the remaining energy consumption covered by the grid is 1998 kWh. The total annual energy produced from solar PV and consumed are 10,854 kWh and 1502 kWh, respectively. This means that 9,082 kWh (about 86% of the energy generated) will be connected to the grid, as shown in Fig. 9.

Effects of relative humidity, temperature, and wind speed

The power output of a PV system is significantly affected by the minimum and maximum ambient temperatures (Temp), wind speed (WS), and relative humidity (RH) (Park et al. 2013; Shrestha et al. 2019). The rise of cells temperature coupled with mismatch losses, dust accumulation, power-point errors, and shading, account for array capture losses (L_c), which is the difference between the reference (Y_R) yield an array yield (Y_F) (Marion et al. 2005; Shiva Kumar and Sudhakar 2015; Atsu et al. 2021). Where Y_F is also known as the final yield of the system. Mathematically, the array capture losses are computed using this expression:

$$L_c = Y_R - Y_F \qquad (17)$$

High humidity, Temp, and WS affect the performance of the PV module adversely. The humidity condenses and creates a deposit on the PV panel at the night and this causes greater deflection of irradiance during the day. The curves of RH, temperature, and WS for the Durban North site showed a similar pattern, as presented in Fig. 10.

The testing and rating of solar panels are usually carried out at about 25 °C and are expected to perform optimally between 15 and 35 °C. However, during the summer, the temperature of solar panels in some areas may be as high as 65 °C (BostonSolar 2021). According to the meteorological information obtained from Solargis, the annual average
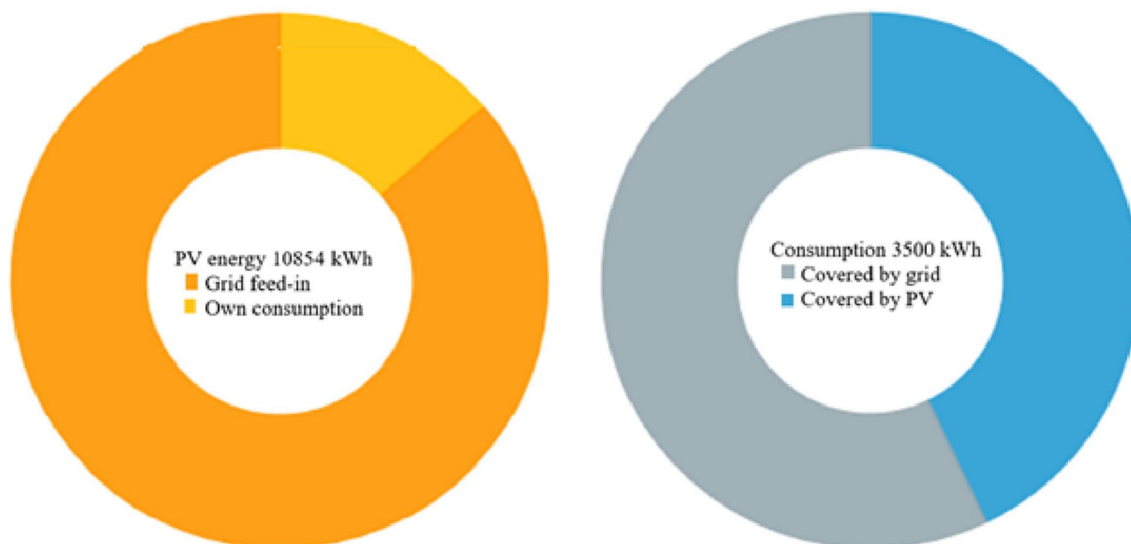
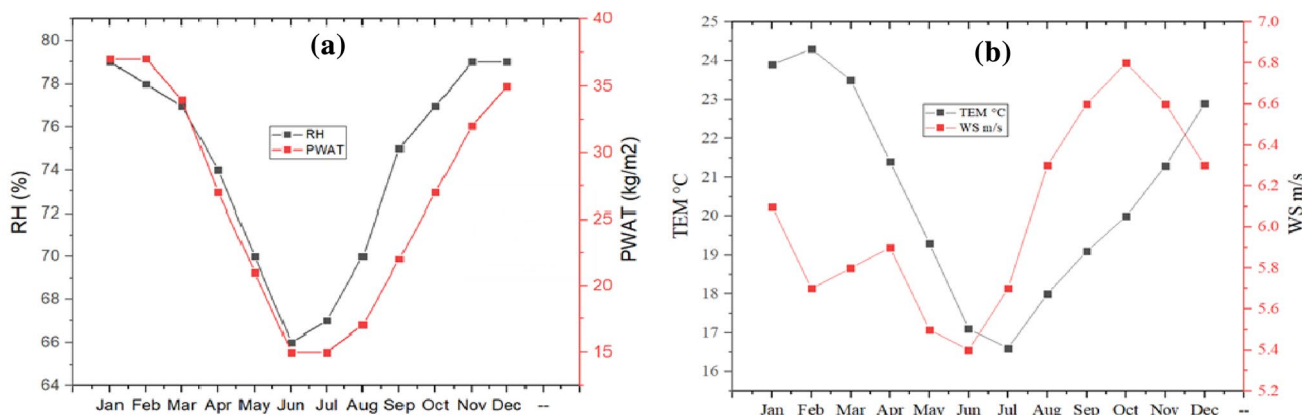**Fig. 9** Energy feed-in grid and energy consumption covered by PV and grid

**Fig. 10** RH, Temp, and WS components of meteorological parameters

temperature of Durban North is 20.6 °C while the lowest (16.6 °C) and highest (24.3 °C) temperatures of Durban North were recorded in July and February, respectively. Further evaluation and analysis of the project-specific meteorological parameters, as presented in Fig. 11, shows that the relation between PR and RH; and PR and temperature are both inverses:

1. The highest PR corresponds to the lowest temperature value. This means that the PV system produces more energy at low temperatures. It implies that the solar PV system is more efficient at low temperatures.
2. The months (June and July) are of a very high PR, which corresponds to the months of a relatively low RH value. This means that the PV system produces more energy when humidity is low. Low humidity causes little limitation to electricity production by the solar PV system.

The efficiency of the PV module is highly affected by the sensitivity of the Si-based PV module to cell temperature. Consequently, there is a notable solar PV system efficiency loss in locations with long hot seasons, due to high temperatures. The negative effects of elevated temperatures on PV systems can be minimized in many ways. These include—leaving few millimeters between the panel and the roof to allow convectional airflow to cool the panels; use of light-colored materials to construct panels to reduce heat absorption; and keep components, such as inverters and combiners under a shaded area behind the array. The influence and relation of other solar PV parameters are presented in Fig. 12.

Where Gi_m is the monthly sum of global irradiation (kWh/m^2), Gi_d is the daily sum of global irradiation (kWh/m^2), Di_d is the daily sum of diffuse irradiation (kWh/m^2) and Ri_d is the daily sum of reflected irradiation (kWh/m^2).

Fig. 11 The graph of RH, Temp, and PR
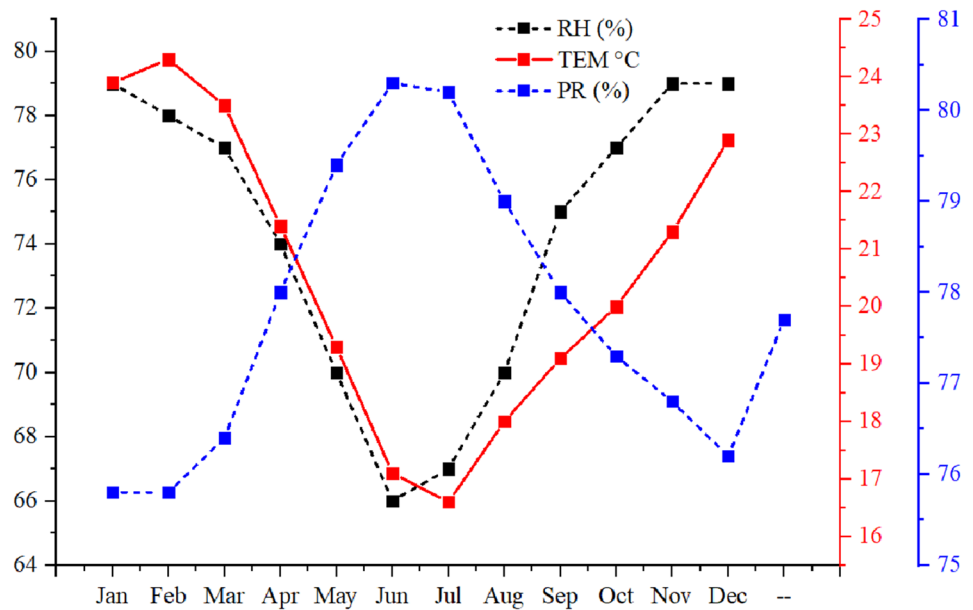
Durban North experiences temperatures between 16.6 and 24.3 °C, rainfall, spectacular thunderstorms, and high humidity that can make muggy days during summer, usually from October to March. These conditions hinder solar PV production performance and that is why the PR in these months is relatively low. In winter (June–August), the condition is different, as the temperature is between 0 and 20 °C and July is the sunniest month with an average temperature of 22 °C. The various weather conditions across the year are shown in Fig. 13a. The southern position in the hemisphere accounts for the times of sunrise and sunset in South Africa. Part of autumn (May) and winter months (June–August) have the longest days, while the summer months (December-February) have the shortest days (Worlddata.info 2021). The Durban average monthly hours of sunshine is represented in Fig. 13(b).

Other PV performance determinants

Many parameters, aside from the ones discussed above, are used to determine the potential of PV and the level of performance of a location and system, respectively. Some of these are the ratio of diffuse horizontal irradiation to global horizontal irradiation (D2G); the Fraction of solar irradiance reflected by surface, the ratio of upwelling to downwelling (GHI) radiative fluxes at the surface, known as surface albedo (ALB). Others are soiling losses and snow losses; the quantification of energy demand needed to cool a building, called cooling degree-days (CDD); and the quantification of energy demand needed to heat a building called heating degree-days (HDD). This study estimated values of these parameters are presented in Table 4.
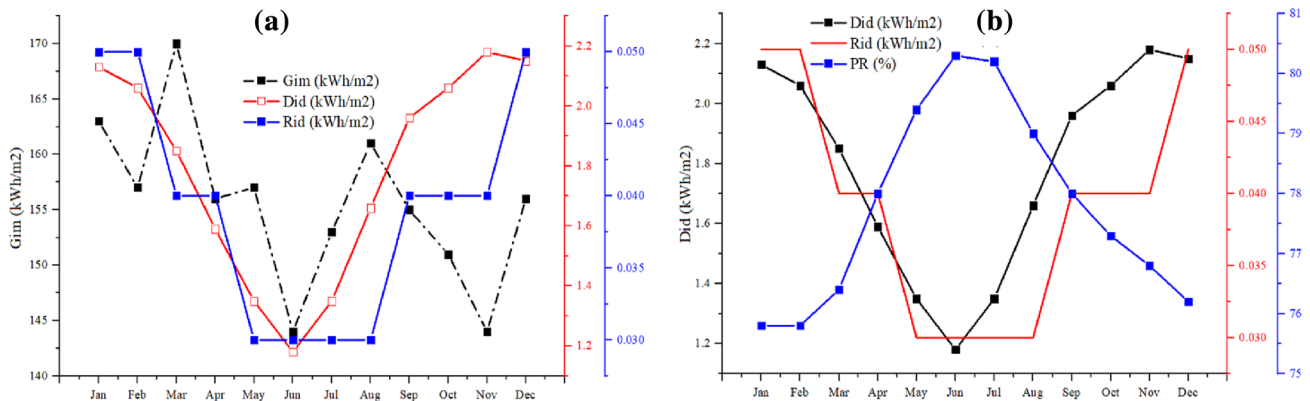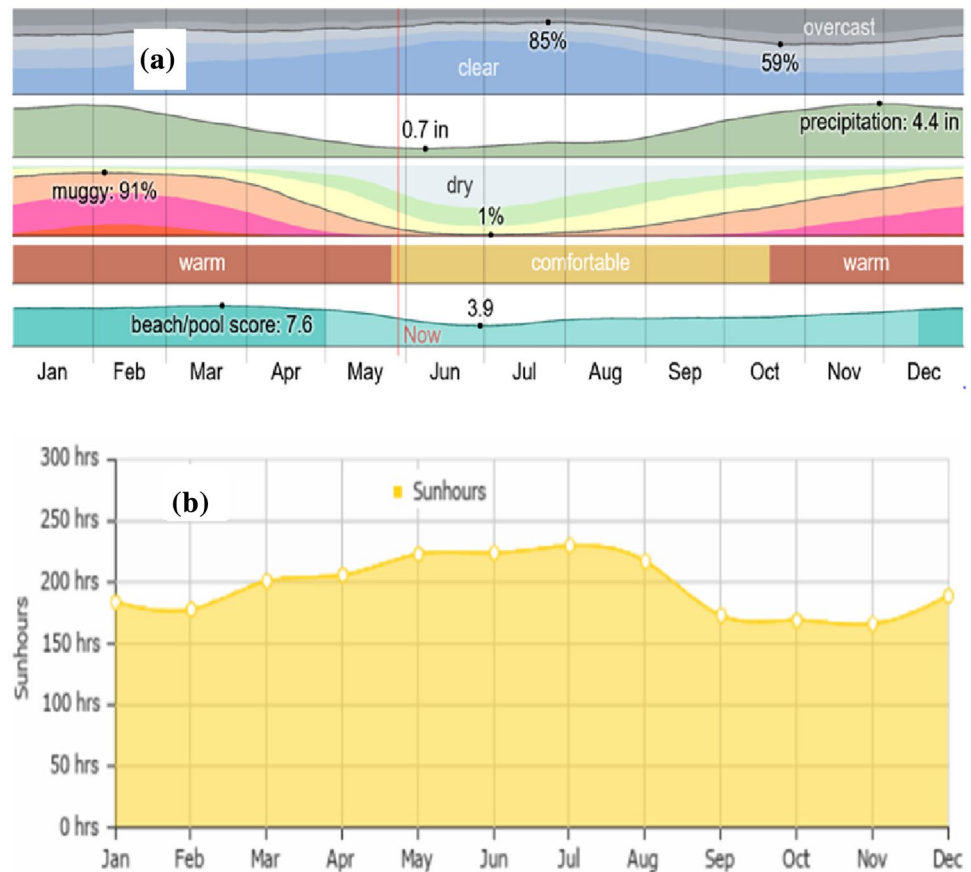

Fig. 12 Effect of humidity on irradiance **a** reflected irradiance; **b** reflected irradiance and PR

Fig. 13 Durban North average monthly hours of sunshine (Weather&Climate 2021)

Evaluation of soiling

The deposition of contaminants, such as dust, snow, dirt, moss, sand, and other particles on surfaces of the PV panels, causes higher absorption and reflection of sunlight. The growth of lichens and mosses and the accumulation of dirt along the frame of the panels can produce partial shadings on the base cells. The droppings from birds pose a serious problem because they cannot be removed by rainfalls. Amongst these contaminants, the dust of typical particle sizes of less than 10 mm in diameter though it depends on the location and environment, is the commonest. Dust is generated from different sources, such as pollution by wind, pedestrians, vehicular movements, and volcanic eruptions. This occurrence reduces solar irradiation, leading to lower energy conversion and yield losses of about 1% or more daily (Ilse et al. 2018); studies have reported that over 50% power reduction possibility by soiling (Sulaiman et al. 2014, Costa, Diniz, and Kazmerski 2018) and soiling effect depends on the nature of the contaminant. Soiling has the following negative effect on the economic revenues of PV installations—reduction in the converted energy by the PV system and increase in the cost of maintenance and operation. This creates further uncertainty on the assessment of PV system performance, prompting higher financial risk and charge of interest rates plant developers. Soiling causes an estimated loss of 4% on the world energy yield of PV and this account for about 2×10^9 USD loss annually (Smestad et al. 2020).

Table 4 PV performance determinants

Month	Jan	Feb	Mar	Apr	May	Jun	Jul	Aug	Sep	Oct	Nov	Dec	Yearly
D2G	0.393	0.372	0.36	0.349	0.325	0.312	0.337	0.37	0.417	0.438	0.447	0.415	0.384
CDD degree days	179	175	172	106	69	37	29	42	44	66	94	143	1155
HDD degree days	0	0	0	0	3	19	32	20	11	1	0	0	87
Soiling losses %	4.5	4.5	4.5	4.5	4.5	4.5	4.5	4.5	4.5	4.5	4.5	4.5	
Snow losses %	0.0	0.0	0.0	0.0	0.0	0.0	0.0	0.0	0.0	0.0	0.0	0.0	

The effect of soiling may be ignored in the middle Europe that experiences medium rainy climates and in residential zones with less than 1%. However, it is important to consider soiling in rural areas with agricultural activities and industrial and railway line zones. The estimation of soiling of PV modules can be done with specialised sensors, a method described as a station-based measurements approach, and directly from the PV energy yield, described as a yield-based approach. Photovoltaic design and simulation software applications, such as PVsyst and Solargis Prospect, are also used to evaluate the effect of soiling on PV performance. The soiling loss (*GL*) is accounted for in terms of irradiance during simulation. In this case, irradiance losses are evaluated as (Zorrilla-Casanova et al. 2013):

$$GL(\%) = \left(\frac{G_{CC} - G_{DC}}{G_{CC}} \right) x100 \tag{18}$$

where G_{CC} is the clean reference solar cell irradiance value measured (W/m^2); and G_{DC} is the dirty reference solar cell irradiance value measured (W/m^2). soiling loss (*GL*).

However, this can be quickly estimated as follow:

1. The region with a long dry season = 5%.

   - Plus 1–2% if the region experiences frequent dust deposition
   - Plus 1% if near a major vehicular traffic area

2. Region with year-round season = 2%.

In this study, an average soiling loss of 4.5% yearly was reported by Solargis Prospect and this amount was uniform in all the months, as presented in Table 4.

Solar PV performance: energy conversion and system losses

The evaluation of the long-term average performance ratio (PR) is important and required for a start-up production of a PV system. The overview of the theoretical yearly specific estimate of solar electricity generation by a PV system, without the long-term aging and performance degradation of PV modules and other system components reflection, are presented in Table 5 and Fig. 8.

The estimation of the energy conversion and losses steps using Solargis PVplanner can be categorized into two components—losses numerically modeled by pvPlanner and losses that are assessed by the user. The integration of these components gives the theoretical losses due to energy conversion in the PV power system, as depicted in Fig. 14.

Economic PV potential: investment consideration parameters

The cost of a PV system depends on on-site location, size and type of installation, type of PV cell technology, and quality of other components. One of the considerations that count in choosing the type of energy to be used is cost. Apart from the conscientious global effort to reduce the use of fossil, the commercial PV panel price decline is mainly responsible for the rapid increase in the deployment of solar PV systems. This section presents financial parameters that are used to establish the investment prospect of a PV system and these include LCOE, IRR, and ROI. The financial parameters inputs required for financial evaluation are presented in Table 6.

Amongst these, derived financial parameters, the simplified LCOE, which describes the cost of generating a unit of energy, is normally used to express the economic potential of solar PV. This is because LCOE connects CAPEX, OPEX, cost of the PV technology, discount rate, and PV plant lifetime. In this study, the calculated LCOE represents the solar PV economic potential by South Africa and the global weighted average CAPEX for a utility-scale PV system of 1,7671 USD/kWh and 1,020 USD/kWh (ESMAP 2020). The estimated IRR project, IRR equity, ROI, and LCOE based on South Africa, and global weighted average CAPEX for the 6-kWp PV system are shown in Fig. 15 shows.

Table 5 System losses and performance ratio

Energy conversion step	Energy output	Energy loss	Performance ratio		
	kWh/ kWp	kWh/ kWp	%	Partial %	Cum. %
Global in-plane irradiation (input)	1873	–	–	100.0	100.0
Global irradiation reduced by terrain shading	1865	− 7	− 0.4	99.6	99.6
Global irradiation reduced by reflectivity	1817	− 48	− 2.6	97.4	97.1
Conversion to DC in the modules	1594	− 224	− 12.3	87.7	85.1
Other DC losses	1506	− 88	− 5.5	94.5	80.4
Inverters (DC/AC conversion)	1469	− 38	− 2.5	97.5	78.4
Transformer and AC cabling losses	1447	− 22	− 1.5	98.5	77.3
Reduced availability	1403	− 43	− 3.0	97.0	74.9
Total system performance	**1403**	− 469	**− 25.1**	–	**74.9**

Fig. 14 The theoretical losses due to energy conversion in the PV power system
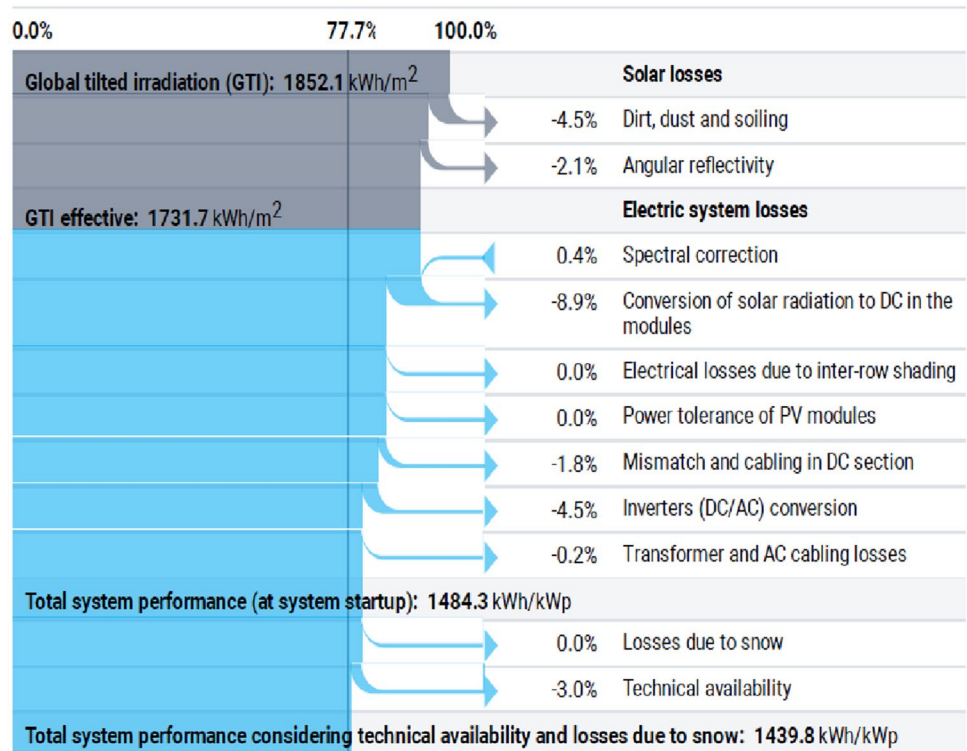
Table 6 Financial inputs

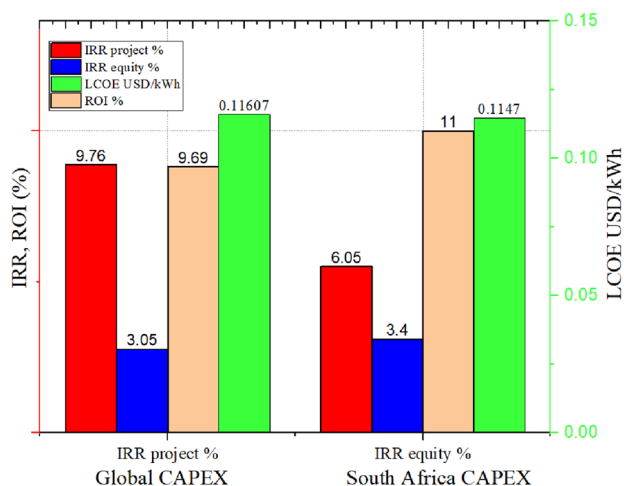| Price of electricity		System installation costs	
Power purchase agreement/Feed-in tariff (USD/kWh)	0.12	Installed capacity (kWp)	6
Tariff indexation rate (%)	0.50	System installation costs (USD)	10,020
Annual operational costs		Unit system costs (USD/kWp)	1,671
Annual operational costs (USD)	150	CAPEX (USD)	10,026
Maintenance reserve account (USD/annually)	70.0	Loan (USD)	13,440
Year of inverter replacement (years)	12.0	Equity (USD)	0
OPEX (USD/annually)	220.0	Debt to equity ratio (%)	134.05
OPEX inflation rate (%)	2.00	Interest rate (%)	3.00
PV system configuration		Loan period (years)	15
Project's years of operation (years)	25.0	Linear loan repayment (USD/annually)	1,125.8
System availability 97.00%		*Accounting information*	
PVOUT_total (year 0) (kWh)	8,653.5	Discount rate (%)	0.00
Degradation first year (%)	0.80	Taxes on profit (%)	10.00
Degradation next years (%)	0.50	Linear tax depreciation (years)	10.0

In December 2020, the price of electricity of 0.145 USD/kWh for households was reported in South Africa while the global average price of electricity was put at 0.136 USD/kWh (GlobalPetrolPrices 2021). In Germany, the LCOE of a rooftop PV system is in the range of 0.053–0.12 USD/kWh, as reported in June 2021 (Kost et al. 2021). Relatively, LCOE of 0.1147 USD/kWh and ROI of 11% in a developing country, such as South Africa is very competitive and viable from a business sense.

Performance comparison

The summary of the technical performance simulation of the solar PV system obtained from the three PV software applications is reported in Table 7. The results obtained from software applications, PV*SOL, Solargis Prospect, and PVplanner, were similar. The outputs from Solargis Prospect and PVplanner were closer, while PV*SOL

Table 7 Summary of results obtained from PV*SOL, and SolarGIS Prospect and PVplanner

PV software application	PV*SOL	SolarGIS-Prospect	SolarGIS-PVplanner
Meteorological parameter			
Global horizontal irradiation (kWh/m^2)	1877	1659.3	1865
Direct normal irradiation (kWh/m^2)		1610.6	
Diffuse horizontal irradiation (kWh/m^2)		636.6	
Air temperature (°C)	15.5	20.6	20.9
Performance parameter			
Annual PV energy (kWh)	10,583	8639	8419
Spec. annual yield (kWh/kWp)	1763.88	1439.8	1403
The month with max energy output	August	March	March
Average PR, (%)	88.89	77.7	74.9
Avoided CO$_2$ emissions (kg/year)	5662		
Solar fraction (%)	42.5		

Fig. 15 The calculated IRR project, IRR equity, ROI, and LCOE based on South Africa and global weighted average CAPEX

Conclusion

The goal of this study is to assess the solar PV Potential and performance of a 6-kWp system grid-connected for a household in site at Durban North, Durban, South Africa. The study is expected to provide information that will facilitate accurate PV system sizing and offer both economic and technical guides to installers and investors. Additionally, policymakers will find this study useful in forming the relevant framework to boost the provision of clean electricity.

Solar PV systems stand out amongst the RE technologies currently being exploited due to their resources distribution, level of advancement, and the degree of resource available for use. Photovoltaic potential and system assessment is an optimisation and a site-based study, which offers both economic and technically relevant information to PV system investors, designers, and installers. Hence, the target of this study is an assessment of solar PV resources and the performance of a grid-connected 6-kWp PV system for household use in a site at Durban North, Durban, South Africa. This will provide accurate and precise data that will facilitate reliable PV design, system installation, and greater deployment of PV systems for clean electricity. Additionally, this study is useful to policymakers in formulating policies and RE roadmap to improve and increase the provision of clean electricity.

A hypothesised monocrystalline solar PV system was used to predict the economic and technical performance parameters of a 6-kWp installed capacity grid-connected rooftop solar PV system to supply electricity to a household. The study was performed using PV*SOL, SolarGIS-Prospect, and SolarGIS-pvPlanner software applications. The parameters evaluated include the yearly average of GHI, DNI, DIF, GTI, TEMP, PVOUT specific, PVOUT total, and PR. Other parameters are energy yield assessment, energy consumption, and electricity feed-in-grid. Variations were

energy output deviates much more, compared to the other two. Solargis Prospect and PVplanner reported March as the month with the highest energy output while PV*SOL shows maximum energy output in August. The rise in temperature causes a decrease in solar PV output; hence, the output in March should be less, while the moderate temperature in August allows energy conversion from the solar PV system. This was observed in PV*SOL energy output only and the PR pattern outputs of both Solargis and PVplanner applications. The PR obtained from PV*SOL is significantly higher than Solargis software applications.

observed in the predicted values in the reports obtained from the different software applications. Some of the parameters that were different were seen are annual energy production, specific annual energy yield, PR, and energy yield. These variations were attributed to the difference in model equations and source of climate data amongst the simulation software applications. However, the absence of checked irradiance data and PV power output restrains the proof of the results. The study presents some valuable perceptions into the rooftop PV system to meet the normal household's energy needs, irrespective of the noted shortcomings. The highlights as obtained from the simulation results are as follows:

1 The reported annual energy yield of 1403 kWh/kWp, shows that the monocrystalline PV module rooftop grid-connected system installations in Durban North of South Africa is a technically viable green energy alternative for residential areas, government buildings, business centers, etc.

2 Depending on the available rooftop area, the PV energy production performance is good with the scope of capacity scale up above 6 kWp in the Durban North region.

3 The annual energy production of 8419 kWh was reported and about 86% of this was fed into the grid.

4 The solar PV system PR of 74.9% obtained is satisfactory for installation and commissioning

5 By using the proposed PV system, an estimated 43% reduction of the annual energy requirement from the electrical grid was obtained.

6 Comparatively, PV*SOL exhibits easy, fast, and most reliable trends as a simulation tool for the solar PV system.

7 The proposed grid-connected rooftop PV system in Durban North is feasible as the results show technical viability, with the benefits of clean energy provision, CO_2 emission reduction, and energy savings.

8 Others are economic performance parameters – levelised cost of energy (LCOE) 0.1147 USD/kWh, internal rate of return (IRR) 17,671 USD/kWh, and return on investment (ROI) 11%.

The results show that the proposed solar PV system under the current conditions is both economically and technically viable for household electrification in Durban North, South Africa.

Future study

An empirical study, as an extension of this research, is required to validate the simulation results. This will include the collection of data through direct measurement of irradiance and the power output of a 6-kWp installed capacity of a monocrystalline silicon rooftop PV system in a sited at Durban North, South Africa.

Declarations

Conflict of interest The authors declare that there is no conflict of interest.

References

Alamoud ARM (2000) Characterization and assessment of spectral solar irradiance in Riyadh, Saudi Arabia. J King Saud Univ – Eng Sci 12(2):245–254. https://doi.org/10.1016/S1018-3639(18)30717-7

Aljazeera (2019) "East Africa struggles with heavy rains as thousands displaced." accessed 18/20/2019. https://www.aljazeera.com/news/2019/11/east-africa-struggles-heavy-rains-thousands-displaced-191129061914721.html

Almasoud AH, Gandayh HM (2015) Future of solar energy in Saudi Arabia. J King Saud Univ - Eng Sci 27(2):153–157. https://doi.org/10.1016/j.jksues.2014.03.007

ArcMap (2020) How solar radiation is calculated. https://desktop.arcgis.com/en/arcmap/10.3/tools/spatial-analyst-toolbox/how-solar-radiation-is-calculated.htm. Accessed 19 Sept 2021

Atsu D, Seres I, Farkas I (2021) The state of solar PV and performance analysis of different PV technologies grid-connected installations in Hungary. Renew Sustain Energy Rev 141:110808. https://doi.org/10.1016/j.rser.2021.110808

BostonSolar. 2021. How do temperature and shade affect solar panel efficiency? In *Boston Solar*.

Carolyn R, Nelson M, Brockman K (2009) "Solar Electric System Design, Operation and Installation: An Overview for Builders in the Pacific Northwest." *Washington State University Extension Energy Program*

Christoph K, Shammugam S, Fluri V, Peper D, Davoodi Memar A, Schlegl T (2021) Evelized cost of electricity renewable energy technologies June 2021. Fraunhofer Institute for Solar Energy Systems ISE

Cioban A, Criveanu H, Matei F, Pop I, Rotaru A (2013) Aspects of solar radiation analysis using ArcGis. Bulletin UASVM Horticulture 70(2):437–440

Costa SCS, Antonia SA, Diniz C, Kazmerski LL (2018) Solar energy dust and soiling R&D progress: literature review update for 2016. Renew Sustain Energy Rev 82:2504–2536. https://doi.org/10.1016/j.rser.2017.09.015

Cotfas, Daniel N/A. "Measurement of Solar Radiation Calibration of PV cells." accessed 19/05/2021. https://slidetodoc.com/measurement-of-solar-radiation-calibration-of-pv-cells/

Daniel KM, Sunter DA "City-Integrated Renewable Energy for Urban Sustainability." The Goldman School of Public Policy, accessed 30/11/2017. https://gspp.berkeley.edu/research/featured/city-integrated-renewable-energy-for-urban-sustainability.

Dondariya C, Porwal D, Awasthi A, Shukla AK, Sudhakar K, Murali Manohar SR, Bhimte A (2018) Performance simulation of grid-connected rooftop solar PV system for small households: a case

study of Ujjain, India. Energy Rep 4:546–553. https://doi.org/10.1016/j.egyr.2018.08.002

ESMAP (2020) Global photovoltaic power potential by country. edited by Global Photovoltaic Power Potential by Country. Energy Sector Management Assistance Program (ESMAP), World Bank, Washington DC

Ebhota WS (2019) Power accessibility, fossil fuel and the exploitation of small hydropower technology in sub-Saharan Africa. Int J Sustain Energy Plan Manage. https://doi.org/10.5278/ijsepm.2019.19.3

Ebhota WS, Tabakov PY (2020) Development of domestic technology for sustainable renewable energy in a zero-carbon emission-driven economy. Int J Environ Sci Technol. https://doi.org/10.1007/s13762-020-02920-9

FloodList (2019a) "DR Congo – 600,000 Affected by Floods in 12 Provinces, Says UN." accessed 18/12/2019. http://floodlist.com/africa/dr-congo-floods-december-2019

FloodList (2019b) "Uganda – More Fatalities After Floods in Central and Eastern Regions." accessed 18/12/2019. http://floodlist.com/africa/uganda-floods-central-eastern-region-december-2019

Fu P, Rich PM (2002) A geometric solar radiation model with applications in agriculture and forestry. Comput Electron Agric 37(1):25–35. https://doi.org/10.1016/S0168-1699(02)00115-1

Fuzen (2021) "List of solar PV design software tools." accessed 03/05/2021. https://www.fuzen.io/solar-epc/list-of-solar-pv-design-software-tools/

GlobalPetrolPrices (2021) "South Africa electricity prices." accessed 14/09/2021. https://www.globalpetrolprices.com/South-Africa/electricity_prices/

Huld T, Waldau AJ, Ossenbrink H, Szabo S, Dunlop E, Taylor N (2014) "Cost maps for unsubsidised photovoltaic electricity." *European Commission*

IEA (2017) Energy Access Outlook: From Poverty to Prosperity. International Energy Agency (IEA), Paris, France

IEA (2021) Global Energy Review: CO2 Emissions in 2020. International Energy Agency, Paris, France

Ilse KK, Figgis BW, Naumann V, Hagendorf C, Bagdahn J (2018) Fundamentals of soiling processes on photovoltaic modules. Renew Sustain Energy Rev 98:239–254. https://doi.org/10.1016/j.rser.2018.09.015

Khatib T, Mohamed A, Sopian K (2012) A software tool for optimal sizing of PV systems in Malaysia. Model Simul Eng 2012:969248. https://doi.org/10.1155/2012/969248

Kost C, Shammugam S, Fluri V, Peper D, Davoodi Memar A, Schlegl T (2021) Levelized cost of electricity renewable energy technologies. June 2021. Fraunhofer Institute for Solar Energy Systems ISE

Li C (2021) Evaluation of the viability potential of four grid-connected solar photovoltaic power stations in Jiangsu Province, China. Clean Technol Environ Policy. https://doi.org/10.1007/s10098-021-02111-1

Marion B, Adelstein J, Boyle K, Hayden H, Hammond B, Fletcher T, Canada B, Narang D, Shugar D, Wenger H, Kimber A, Mitchell L, Rich G, Townsend T (2005) "Performance parameters for grid-connected PV systems." Conference Record of the Thirty-first IEEE Photovoltaic Specialists Conference, 2005., 3–7

NREL (2016) Transforming Energy through Science. In *NREL Fact Sheet*. National Renewable Energy Laboratory, Office of Energy Efficiency and Renewable Energy, USA

Nachmany M, Fankhauser S, Townshend M, Collins T, Landesman T, Matthews A, Pavese C, Rietig K, Schleifer P, Setzer J (2014) "The Globe Climate Legislation Study: A Review of Climate Change Legislation in 66 Countries." *Globe International and the Grantham Research Institute, London School of Economics, London*

Njoku HO, Omeke OM (2020) Potentials and financial viability of solar photovoltaic power generation in Nigeria for greenhouse gas emissions mitigation. Clean Technol Environ Policy 22(2):481–492. https://doi.org/10.1007/s10098-019-01797-8

Park NC, Oh WW, Kim DH (2013) Effect of temperature and humidity on the degradation rate of multicrystalline silicon photovoltaic module. Int J Photoenergy 2013:925280. https://doi.org/10.1155/2013/925280

Quansah DA, Adaramola MS, Appiah GK, Edwin IA (2017) Performance analysis of different grid-connected solar photovoltaic (PV) system technologies with combined capacity of 20 kW located in humid tropical climate. Int J Hydrogen Energy 42(7):4626–4635. https://doi.org/10.1016/j.ijhydene.2016.10.119

Rich PM, Dubayah R, Hetrick WA, Saving SC (1994) "Using viewshed models to calculate intercepted solar radiation: applications in ecology." *American Society for Photogrammetry and Remote Sensing Technical Papers*:524–529

Rinaldi F, Moghaddampoor F, Najafi B, Marchesi R (2021) Economic feasibility analysis and optimization of hybrid renewable energy systems for rural electrification in Peru. Clean Technol Environ Policy 23(3):731–748. https://doi.org/10.1007/s10098-020-01906-y

Roadmap (2020) "Technology-Roadmap: Solar Photovoltaic (PV) Roadmap for Singapore." accessed 11/05/2021. https://www.nccs.gov.sg/media/publications/technology-roadmap

Sean F (2019) "Chart of the day: These countries create most of the world's CO2 emissions." accessed 15/09/2021. https://www.weforum.org/agenda/2019/06/chart-of-the-day-these-countries-create-most-of-the-world-s-co2-emissions/

Shiva Kumar B, Sudhakar K (2015) Performance evaluation of 10 MW grid connected solar photovoltaic power plant in India. Energy Rep 1:184–192. https://doi.org/10.1016/j.egyr.2015.10.001

Shrestha AK, Thapa A, Gautam H (2019) Solar radiation, air temperature, relative humidity, and dew point study: Damak, Jhapa, Nepal. Int J Photoenergy 2019:8369231. https://doi.org/10.1155/2019/8369231

Smestad GP, Germer TA, Alrashidi H, Fernández EF, Dey S, Brahma H, Sarmah N, Ghosh A, Sellami N, Hassan IAI, Desouky M, Kasry A, Pesala B, Sundaram S, Florencia Almonacid KS, Reddy TK, Mallick, and Leonardo Micheli. (2020) Modelling photovoltaic soiling losses through optical characterization. Sci Rep 10(1):58. https://doi.org/10.1038/s41598-019-56868-z

Sulaiman SA, Singh AK, Mokhtar MMM, Bou-Rabee MA (2014) Influence of Dirt Accumulation on Performance of PV Panels. Energy Procedia 50:50–56. https://doi.org/10.1016/j.egypro.2014.06.006

Thomas EJ (2014) Nuclear Energy: The Safe, Clean, Cost-Effective Alternative. The Objective Standard, Fall 2013 8(3). https://theobjectivestandard.com/2013/08/nuclear-energy-safe-clean-cost-effective/

UN (2015) "Resolution adopted by the General Assembly on 25 September 2015." United Nations New York

WEC (2013) World Energy Resources: Solar World Energy Council

Weather&Climate (2021) "Climate in Durban (KwaZulu-Natal), South Africa." accessed 25/05/2021. https://weather-and-climate.com/average-monthly-Rainfall-Temperature-Sunshine,durban,South-Africa

Williams ES, Jen T-C (2018) "Photovoltaic solar energy: potentials and outlooks." ASME International Mechanical Engineering Congress and Exposition, Pittsburgh, Pennsylvania, USA

Wolf E (2015) Chapter 9-Large-scale hydrogen energy storage. In: Moseley PT, Garche J (eds) Electrochemical energy storage for renewable sources and grid balancing. Elsevier, Amsterdam, pp 129–142

Worlddata.info. (2021) "Sunrise and sunset in South Africa." accessed 28/05/2021. https://www.worlddata.info/africa/south-africa/sunset.php

Worldmeter (2020) "CO$_2$ Emissions." accessed 15/09/2021. https://www.worldometers.info/co2-emissions/

Worldmeter (2021) "South Africa CO$_2$ Emissions." accessed 15/09/2021. https://www.worldometers.info/co2-emissions/south-africa-co2-emissions/

Zorrilla-Casanova J, Piliougine M, Carretero J, Bernaola-Galván P, Carpena P, Mora-López L, Sidrach-de-Cardona M (2013) Losses produced by soiling in the incoming radiation to photovoltaic modules. Prog Photovoltaics Res Appl 21(4):790–796. https://doi.org/10.1002/pip.1258

Authors and Affiliations

Williams S. Ebhota[1] · **Pavel Y. Tabakov[1]**

✉ Williams S. Ebhota
williame@dut.ac.za

[1] Department of Mechanical Engineering, Institute for Systems Science, Durban University of Technology, Durban, South Africa